Food and Chemical Toxicology 132 (2019) 110654

Contents lists available at ScienceDirect

Food and Chemical Toxicology

journal homepage: www.elsevier.com/locate/foodchemtox

Cucurbitacin IIa interferes with EGFR-MAPK signaling pathway leads to proliferation inhibition in A549 cells

Jie Zhang[a], Yifan Song[a], Yuan Liang[a], Haoyang Zou[a], Peng Zuo[b], Mi Yan[a], Siyuan Jing[a], Tiezhu Li[b], Yongjun Wang[b], Da Li[b], Tiehua Zhang[a,*], Zhengyi Wei[b,**]

[a] College of Food Science and Engineering, Jilin University, Changchun, 130062, China
[b] Institute of Agricultural Biotechnology, Jilin Academy of Agricultural Sciences, Changchun, 130033, China

ARTICLE INFO

Keywords:
Epidermal growth factor receptor
Cucurbitacin
Apoptosis
Cell cycle arrest
Molecular simulation

ABSTRACT

Cucurbitacin IIa (CuIIa), a tetracyclic triterpenoid harboring anticancer activity, was investigated in A549 cells to reveal its mechanism of targeting on epidermal growth factor receptor (EGFR) signaling pathway. Results showed that CuIIa was capable of inducing apoptosis and cell cycle arrest at G2/M phase. The transcription of EGFR pathway genes and their proteins accumulation was inconsistently influenced by CuIIa. Notably, transcription of *Raf1* was significantly upregulated, nevertheless, *MEK1* and *ERK1* were significantly downregulated. On the other hand, the accumulation of the total and phosphorylated proteins of the most members in EGFR-mitogen-activated protein kinase (MAPK) pathway, as well as CylclinB1 and survivin were also shifted by CuIIa treatment. Remarkably, total MEK remained constant but survivin completely degraded. Moreover, phosphorylated BRAF continuously increased while Raf1 and MEK decreased continuously. CuIIa was further confirmed to be a tyrosine kinase inhibitor (TKI) of EGFR by kinase inhibition assay. The results of molecular simulation showed that the long side chain of CuIIa occupied the binding pocket of EGFR and the ligand was stabilized at the active site of EGFR. In view of the results above, it is suggested that CuIIa inhibits cell proliferation by interfering the EGFR-MAPK signaling pathway.

1. Introduction

Epidermal growth factor receptor (EGFR), also known as ErbB1 and HER, belongs to the ErbB family and is a typical receptor tyrosine kinase (RTK) (Wheeler et al., 2008). EGFR is activated by binding with ligands and plays essential roles in cell proliferation, differentiation, migration, and apoptosis by exciting the subsequent intracellular signaling pathways (Kampa-Schittenhelm et al., 2013; Lemmon and Schlessinger, 2010; Yarden and Sliwkowski, 2001). There are two primary EGFR downstream signaling pathways, the PI3K/Akt/PTEN/mTOR and the RAS/RAF/MEK/ERK (Ellis, 2004). Upon binding with ligands such as epidermal growth factor (EGF), EGFR transforms into homodimer or heterodimer by dimerizing with itself or other ErbB family members, and triggers the downstream signaling (Arteaga, 2001; Ellis, 2004). It is demonstrated that overactivation of EGFR pathways results in numerous malignant tumors, e.g., non-small cell lung cancer (NSCLC) (Liu et al., 2018b). Thus, EGFR is an essential target in clinic cancer therapy (Nakai et al., 2016; Padfield et al., 2015; Saada-Bouzid and Le Tourneau, 2019), especially in NSCLC therapy (Cheng and Chen, 2014; Dong et al., 2019; Kim et al., 2019; Lee, 2017; Martinelli et al., 2017; Masri et al., 2018; Rotow and Bivona, 2017). Numerous of tyrosine kinase inhibitors (TKIs) have been developed to treat the EGFR pathway related tumors and benefit the patients harboring cancer with EGFR mutations (Liu et al., 2018b). These TKIs are small molecules either natural or artificially synthesized.

Cucurbitacins, a class of tetracyclic triterpenoids from Cucurbitaceae plants, are divided into twelve categories with over 200 derivatives. Numerous cucurbitacins such as cucurbitacin B, E, I, Q, and IIa have been reported to exhibit various biological activities (Ahmed and Halaweish, 2014; Alsayari et al., 2018; Cai et al., 2015; Chen et al., 2012; Ganesan et al., 2018; Kaushik et al., 2015; Liang and Chen, 2019; Price et al., 1987; Seo et al., 2014). They exert the anticancer activity by inducing apoptosis, autophagy and cell cycle arrest (Cai et al., 2015). EGFR signaling pathway is one of the targets for the cucurbitacins. Cucurbitacin A (CuA) is reported to inhibit the expression of genes involved in PI3K/AKT/mTOR signaling pathway in ovarian cancer cells SKVO3 (Liu et al., 2018a). It is also found that CuA treatment inhibited mTOR/PI3K/AKT signaling pathway, thus inducing cell cycle arrest in

* Corresponding author.
** Corresponding author.
E-mail addresses: zhangthjlu@163.com (T. Zhang), weizy80@163.com (Z. Wei).

https://doi.org/10.1016/j.fct.2019.110654
Received 28 April 2019; Received in revised form 25 June 2019; Accepted 29 June 2019
Available online 29 June 2019

NSCLC A549 cells (Wang et al., 2017). It is reported that cucurbitacin B (CuB) induces apoptosis and cell cycle inhibition by inhibiting the STAT3 and EGFR signaling in colorectal cancer cells HT-29 and HCT-116, and the efficacy is reported to be better when CuB is combined with the orally active inhibitor of EGFR, gefitinib (Yar Saglam et al., 2016). CuB is capable of suppressing both wildtype- (A549 and H1792) and mutant- (H1560 and H1975) EGFR lung cancer cells via inhibition of PI3K/mTOR and STAT3 signaling (Khan et al., 2017). Treatment with CuB showed that the expression of EGFR and the proteins in downstream signaling pathways were inhibited, such as PI3K/AKT/mTOR and STAT3. Moreover, the signaling of EGFR, PIK/AKT/mTOR, and STAT3 were significantly inhibited by combined treatment with CuB and ERK inhibitor in pancreatic cancer cells (Zhou et al., 2017). According with a study by Lopez-Haber and Kazanietz, cucurbitacin I (CuI) inhibited the motility and Rac1 activation by EGFR (ErbB) in breast cancer cell and the ErbB-driven Rac1 activation in breast cancer cells was independent from the JAK2/STAT3 pathway (Lopez-Haber and Kazanietz, 2013). CuI inhibited the cell growth of human NSCLC cells by inhibiting of the PI3K/AKT/p70S6K signaling pathway (Lopez-Haber and Kazanietz, 2013). Interestingly, CuI inhibited the phosphorylation of STAT3 through this pathway but meanwhile enhanced the phosphorylation of STAT1.

Although the mechanisms of several cucurbitacins in cancer cells have been illustrated (Alsayari et al., 2018; Cai et al., 2015; Garg et al., 2018; Liang and Chen, 2019), how cucurbitacin IIa (CuIIa) works in anticancer activity is rarely reported. It is reported that CuIIa induced the irreversible clusterization of filamentous actin and arrested cell cycle at in G2/M phase in the cell lines of hepatocellular carcinoma H22 (mouse), lung cancer (human) NCI–H1299, and prostate cancer PC-3 and CWR22Rv-1 (human) (Boykin et al., 2011). CuIIa induced apoptosis by inhibiting survivin independent of JAK2/STAT3 phosphorylation (Boykin et al., 2011). In other work (He et al., 2013), CuIIa was found to induce caspase-3-dependent apoptosis via increasing caspase-3 cleavage and survivin degradation, thus enhancing autophagy in lipopolysaccharide-stimulated RAW 264.7 macrophages. Surprisingly, to date, although EGFR pathway is a hot topic in drug exploration for cancer therapy, few reports are available on impact of CuIIa with this pathway. CuIIa, however, is reported to be capable of inhibiting the proliferation of cancer cells (Boykin et al., 2011; Wu et al., 2002).

The interactions of numerous natural or synthetic TKIs to EGFR have been described (Chung et al., 2011; Hu et al., 2017; Li et al., 2012a, 2012b, 2015). Although several cucurbitacins have been confirmed to interfere the EGFR signaling pathway, how the cucurbitacin molecules interact with the targets (e.g., EGFR) to exert their activity of inhibiting the proliferation (growth) of cancer cells still remains unclear, and only a few reports are available on the interaction mechanism of cucurbitacin derivatives (Mahnashi et al., 2019; Zubair et al., 2016).

In this paper, we present a fact that CuIIa interferes the EGFR-mitogen-activated protein kinase (MAPK) signaling by affecting the transcription, accumulation and phosphorylation of the signaling participants. The impaired signaling results in apoptosis and arrests the cell cycle at G2/M phase. CuIIa is also proved to be capable of inhibiting the kinase activity of EGFR. The results of molecular simulation show that the long side chain of CuIIa occupies the binding pocket of EGFR and the ligand is stabilized at the active site of EGFR.

2. Materials and methods

2.1. Materials

Non-small cell lung cancer cell line A549 was purchased from the Cell Bank of the Chinese Academy of Sciences (Shanghai, China). Dulbecco's modified eagle's medium (DMEM), 0.25% trypsin solution (with EDTA), dimethyl sulfoxide (DMSO), methylthiazolyldiphenyl-tetrazolium bromide (MTT) assay kit, penicillin and streptomycin were purchased from Solarbio Life Science Ltd. (Beijing, China). Fetal bovine serum (FBS) was from HyClone (Logan, UT, USA). Roswell Park Memorial Institute (RPMI) 1640 was purchased from Biological Industries Ltd. (Kibbutz, Israel). The eBioscience™ Annexin V-FITC Apoptosis Detection Kit and propidiumiodide (PI) were purchased form Thermo Fisher Scientific (San Jose, CA, USA). Staurosporine was purchased from Aladdin (Shanghai, China) and HTRF KinEASE-TK kit was purchased from Cisbio Bioassays (Codolet, France).

Trizol reagent, reverse transcriptional kit (TransScript First-Strand cDNA Synthesis SuperMix) and quantitative PCR kit (TransStart Top Green qPCR SuperMix) and Ribonulease A (RNase A) were purchased from Transgen Biotech Ltd. (Beijing, China). Primary antibodies for EGFR and pEGFR (Tyr1068) were purchased from Cell Signaling Technology Inc. (Beverley, MA, USA). Primary antibodies for Raf1 and pRaf1(Ser338), BRAF and pBRAF (Thr401), MEK1/2 and pMEK1/2 (Ser218/Ser222),ERK1/2 and pERK1/2 (Thr202/Tyr204), STAT3, survivin and GADPH were purchased from Abcam Co. (Cambridge, UK). EGFR protein was purchased from Thermo Fisher Scientific (San Jose, CA, USA). HPR-conjugated secondary antibody was purchase from Sino Biological Inc. (Beijing, China) and ECL Immunoblotting Detection Reagents were purchased from Clinx Science Instrument Co., Ltd. (Shanghai, China). CuIIa was purchased from Yuanye Biotechnology Co., Ltd. (Shanghai, China). All the chemical reagents used in the cell culture experiments are cell culture grade.

2.2. Cell culture and MTT assay

A549 cells were cultured in 10 mL DMEM with 100 $mg{\cdot}L^{-1}$ of penicillin and 100 $IU{\cdot}L^{-1}$ of streptomycin supplemented with 10% FBS in 10 cm discs in 37 °C with 5% CO_2 in incubator, approximately 2.5×10^6 cells per disc. Cells were transferred every 4 days with two medium renewals every day after the transfer.

Ten thousand cells were cultured in each well of 96-well plate in 100 μL DMEM for approximately 15 h (to the logarithmic phase), then new medium (100 μL) was replaced and cultured for 1 h. One microliter of CuIIa with different concentrations (4, 5, 6, 7 and 8 mM respectively in DMSO) was added to cell cultures, 3 duplicates per each concentration, then the plate was gently shaken to mix the reagents. DMSO was applied as vehicle contrast (1%, v/v). The cells were cultured for 36h before MTT solution was supplemented. The medium was removed and 90 μL new DMEM and 10 μL MTT solution were applied to each well, and the plate was incubated in the incubator for 4 h. The supernates were disposed and 150 μL of DMSO was added to dissolve formazan and then 570 nm absorption was read using the iMARK microplate reader (Bio-Rad Laboratories, Inc., Hercules, CA, USA), the data was then normalized to the DMSO treatment.

2.3. Apoptosis and cell cycle analysis

Cells were cultured in 6-well plate in 2 mL of RPMI 1640 medium with 10% FBS (2.5×10^5 cells per well) for approximately 15h, then the medium was discarded and 2 mL of new medium was added to each well and subsequently cultured for one hour before 20 μL of 6 mM CuIIa was supplemented. The cells were cultured for 36 h and harvested for apoptosis analysis. Three duplicates were carried out and DMSO was applied as vehicle contrast (1%, v/v). Apoptosis analysis was performed according to the instruction of the Annexin V-FITC Apoptosis Detection Kit. Briefly, the cells were treated with trypsin solution and harvested by centrifugation at 1000 rpm for 5 min. After being rinsed twice with PBS buffer and subsequently centrifugated, the cells from each well were resuspended in 200 μL of binding buffer. Five microliters of Annexin V-FITC were added to the above suspensions, well mixed, and then incubated at room temperature for 10 min. After the incubation, the cells were centrifuged to discard the excessive Annexin V-FITC and rinsed with 200 μL of binding buffer. The cells were then gathered and resuspended with 190 μL of binding buffer, and well mixed with 10 μL

Table 1
Genes tested and primers.

Gene	Accession number	Primers
EGFR	NM_005228	EGFRF: AACCCCGAGGGCAAATACAG EGFRR: AGGCCCTTCGCACTTCTTAC
Raf1	NM_001354695	Raf1F: CCGAGAGTCTTAATCGCGGG Raf1R: CATCGTAGCAAACGCGCTC
BRAF	NM_001354609	BRAFF: ATTTGGGCAACGAGACCGAT BRAFR: GTTGATCCTCCATCACCACGA
MEK1	NM_002755	MEK1F: GAGCCGGAGGGACTGGTTG MEK1R: CCGGTAGCGGTCTCAGTGG
MEK2	XM_006722799	MEK2F: CTACATGGCTCCACCTCCTAAG MEK2R: CCAGCCGGCAAAATCCAC
ERK1	NM_001109891	ERK1F: CCACATTCTGGCCCTTGACC ERK1R: CGCTCCTTAGGTAGGTCATCC
ERK2	NM_002745	ERK2F: GTTCTTGACCCCTGGTCCTG ERK2R: TACATACTGCCGCAGGTCAC
STAT3	XM_017024973	STAT3F: CCAGTCCGTGGAACCATACA STAT3R: GCCTGGGTCAGCTTCAGG
survivin	NM_001012271	SurvF: TCTGTCACGTTCTCCACACG SurvR: GACCTCCAGAGGTTTCCAGC
CyclinB1	NM_031966	CCB1F: AATGGGAAGGGAGTGAGTGC CCB1R: GAGAAGCAGAACACCGGAGG
GADPH	NM_001289745	GADPHF: GAAGACGGGCGGAGAGAAAC GADPHR: GCCCAATACGACCAAATCCG

of PI solution. The mixtures were incubated at room temperature for 15 min and subsequently analyzed with the guava easyCyte™ flow cytometer (EMD Millipore, Inc., Germany). Untreated cells undergone the same operation are adopted as blank control.

2.4. Gene expression assessments

Cells culture and CuIIa treatment were the same as the method for apoptosis analysis. The cells were harvested for total RNAs extraction after treated for 1, 2, 3, 4 and 5 h. Three duplicates were performed for each treatment time and DMSO was applied as vehicle contrast (1%, v/v). Total RNAs were extracted using the Trizol reagent according to the user's manual and 500 ng total RNAs from each sample was used for reverse transcription according to the instruction of the kit. Ten times dilutions of cDNAs were prepared and 1 μL of each sample was used as templates for the quantitative PCR (qPCR) following the product manual. Three duplicates were displayed for each sample. The genes tested and primers used are listed in Tables 1 and 1 μL per each (10 nM) was used in a 20 μL reaction. The PCRs were displayed with the fluorescence quantitative thermocycler using the following parameters: firstly, predenaturation at 94 °C for 10 min; then 40 circles of denaturation at 94 °C for 5 s and annealing at 60 °C for 30 s; after that dissociation at 94 °C for 10 s, 65 °C for 60 s and 97 °C for 10 s and eventually cooling to 37 °C for 30 s. The expression level was calculated by the $^{\Delta\Delta}$Ct methods referenced to the GADPH encoding gene. The expression with $^{\Delta\Delta}$Ct value smaller than −1.0 or greater than 1.0 was considered as significant.

2.5. Immunoblotting analysis

Cells were cultured in 10 cm discs in 10 mL of DMEM (5×10^6 cells per well) for approximately 15 h, then the medium was discarded and 10 mL of fresh DMEM was added to the cells. One hour later, 100 μL of 6 mM CuIIa was supplemented to the cells. The cells were harvested for protein extraction after 1, 2, 4, 8, 12, and 24 h respectively. DMSO was applied as vehicle contrast (1%, v/v). Thirty micrograms of total proteins were loaded to display SDS-PGAE. The accumulation of EGFR, Raf-1, B-Raf, MEK1/2 and ERK1/2, either phosphorylated or not, were tested. The accumulation of STAT3, cyclinB1 and survivin were detected as well. GADPH was adopted as loading control. The proteins above were probed with the respective primary antibody and chemiluminescence was detected with Chemigel6000 Touch imaging system (Clinx Science Instrument Co., Ltd, Shanghai, China) using ECL Immunoblotting Detection Reagents. The relative accumulations of the proteins were quantified by calculating the gray densities of the blots, referencing to GADPH.

2.6. Kinase inhibition assay

The kinase inhibition assay was performed with the homogeneous time-resolved fluorescence (HTRF) method using the HTRF KinEASE-TK kit following the user's manual. Briefly, the enzymatic reaction was started by addition of ATP to a mixture of CuIIa, substrate-biotin and EGFR and incubated at room temperature for 40 min, and the concentration of the reaction components was as advised. The enzymatic reaction was stopped by EDTA-containing buffer with Streptavidin-XL665 and TK Antibody-cryptate. After incubating 1h at room temperature, the plate was read with excitation of 320 nm and emission of 620 and 665 nm on a microplate reader Tecan Infinite® M1000 pro (Tecan, Austria) and calculated into ratio. Ratio = (Signal 665 nm/Signal 620 nm) × 10^4. Statistical analysis and curve fitting were performed using GraphPad Prism 5 (GraphPad Software, La Jolla, CA, USA). Data were presented as mean ± SEM.

2.7. Molecular docking

The three-dimensional structure of the human epidermal growth factor receptor (EGFR) kinase domain with the inhibitor erlotinib (PDB entry code 1M17) was downloaded from the Protein Data Bank (Stamos et al., 2002). Protein preparation was performed by removing erlotinib as well as the water molecules, and then the hydrogen atoms were added. The initial structure of CuIIa was constructed using GaussView and optimized with Gaussian 09W. In order to verify the docking procedure, the original X-ray erlotinib was re-docked back into the binding site of EGFR using AutoDockTools. Then CuIIa was docked into the binding pocket. We performed 10 independent docking runs and the pose with lowest docking energy score was selected for MD simulation.

2.8. Molecular dynamics simulation

To assess the binding stability of CuIIa in the tyrosine kinase domain of EGFR, molecular dynamics simulation was carried out in GROMACS 2019 with the CHARMM36 all-atom force field. The force field parameters of CuIIa were generated with the CGenFF server. The EGFR-CuIIa complex was solvated in a cubic box with simple point charge water molecules at 2 nm marginal radius. After adding counterion to neutralize the charge, the system was submitted for energy minimization. With position restraints on both EGFR and CuIIa, the system was subjected to a 100-ps NVT equilibration simulation and a 100-ps NPT equilibration simulation. Finally, the position restraints were released and subsequently unrestraint production molecular dynamics was run for 20 ns. The root mean squared deviation (RMSD) values of EGFR and CuIIa compared with their respective protein crystal (PDB entry code 1M17) and initial docking structures were calculated.

3. Results and discussion

3.1. CuIIa inhibited A549 cells by inducing apoptosis and cell cycle arrest

The cytotoxic effect of CuIIa on A549 cells was confirmed by MTT assay. CuIIa exhibited anticancer activity by inhibiting proliferation of A549 cells and arrest the cell cycle (Fig. 1). The cytotoxicity was dose dependent, and the IC_{50} value was approximately 60 μM at 36 h. The growth rates were less various around this dose, but there existed sharp gaps when the gaps of the dose increased (Fig. 1A).

Further analysis was carried out to reveal how CuIIa inhibited the proliferation of A549 cells. Annexin V-FITC/PI method was adopted to perform apoptosis analysis. As shown in Fig. 1B, CuIIa was capable of

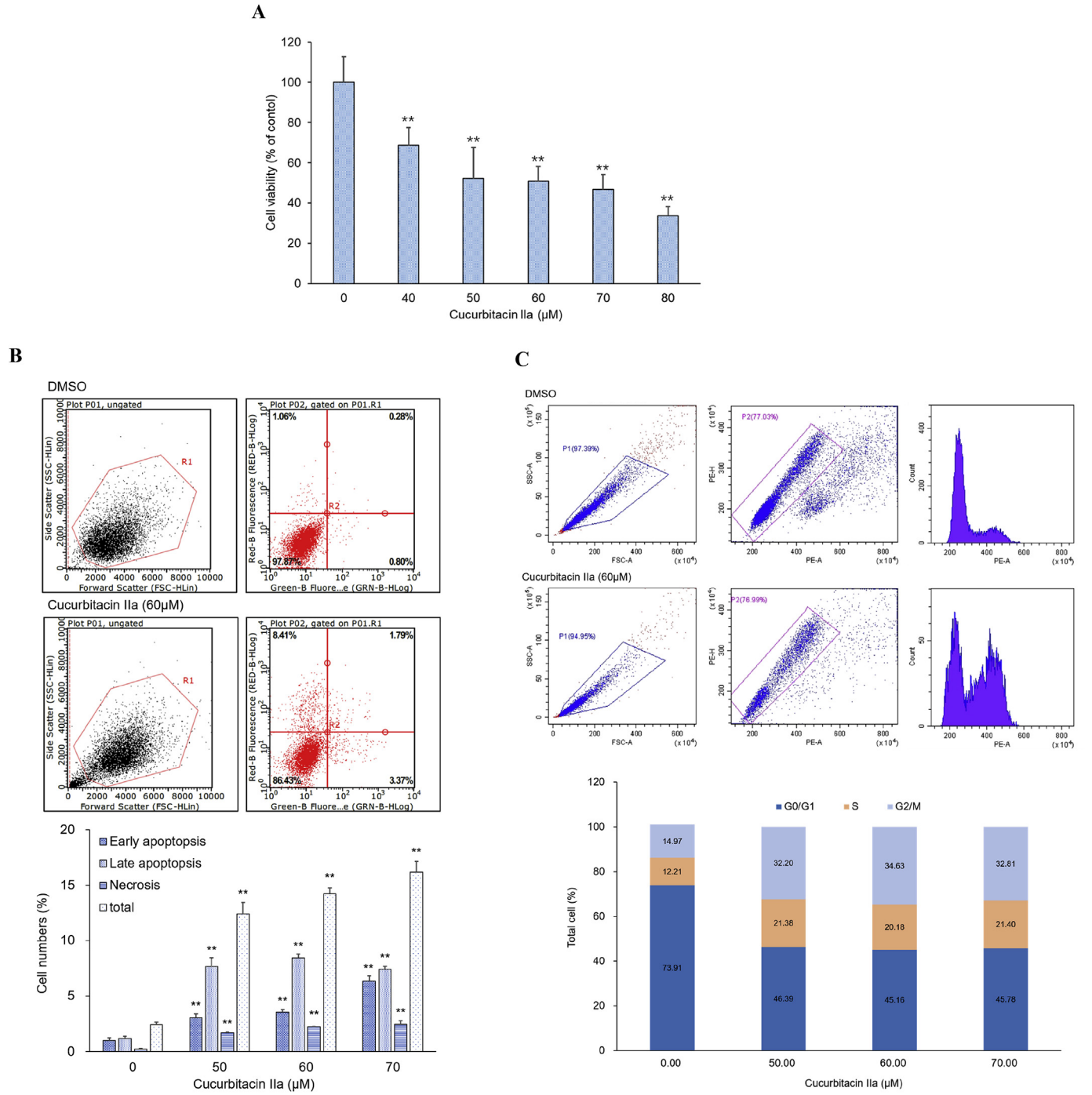

Fig. 1. Cytotoxicity (A), apoptosis (B), and cell cycle (C) analysis of CuIIa to A549 cells. Cytotoxicity assay was based on 1×10^4 cell per well precultured for 15 h in 100 μL medium on 96-well plate treated with various concentrations of CuIIa for 36 h. Apoptosis and cell cycle analysis were performed with 2.5×10^5 cells per well precultured for 15 h in 2 mL medium on 6-well plates treated with 50, 60 or 70 μM of CuIIa. DMSO treatments were used as controls. The Annexin V-FITC/PI method and PI staining method were used for apoptosis and cell cycle analysis respectively. One of DMSO and one of CuIIa (60 μM) treatments were shown as examples to show the gating strategy and flow cytometric charts in the upper parts of B and C. All the data are from three independent repeats per treatment and presented as mean ± SD. **Statistically extremely significant difference ($p < 0.01$).

inducing apoptosis. The induction ability was dose dependent. Although cell viability is not significantly diverse, the status for apoptosis is rather different at the three tested concentrations (50, 60 and 70 μM respectively). The number of cells at early apoptosis and necrosis stage were increased as the doses increased, however the cells in late apoptosis stage reached to a peak at the dose of the IC_{50} value. The total apoptosis cells varied from 12.38% to 16.16%, in which those at late apoptosis stage occupied the largest share. All the numbers, those of cells at early and late stage apoptosis, necrosis and the total, were extremely significant diverse from those of the DMSO vehicles treatment ($P < 0.01$).

Cell cycle analysis was also performed by PI staining method. The cycle was arrested at G2/M phase, and the cell population at this stage increased and occupied around one third of the total cells (Fig. 1C). The percentage of S phase cell population was also increased to around 21% and by contrast, the share of G0/G1 phase cell population reduced to

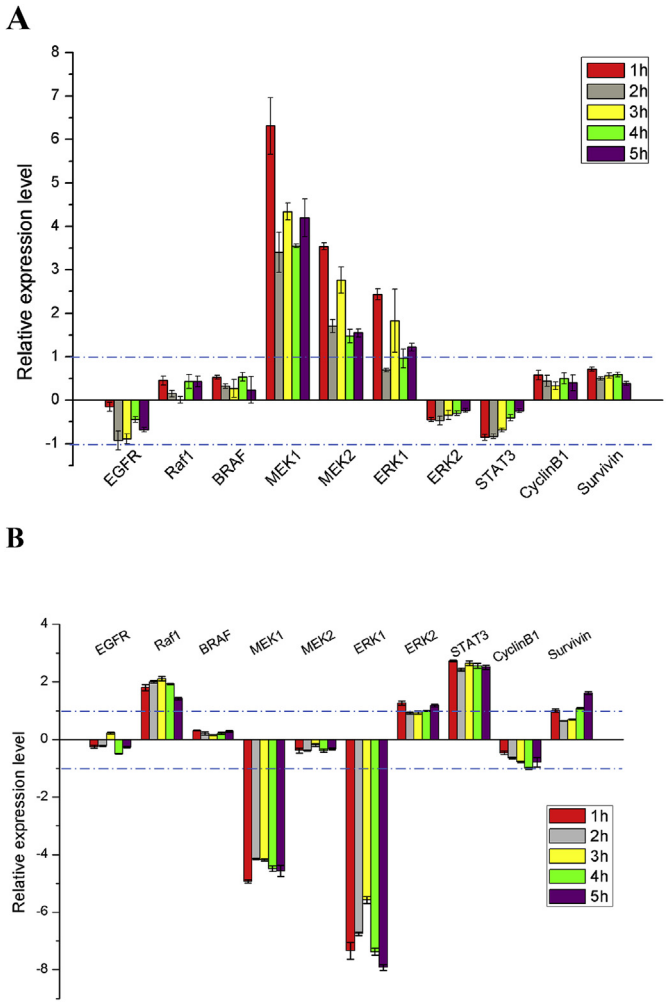

Fig. 2. Transcription patterns of EGFR signaling pathway genes in treatments of DMSO (A) and CuIIa (B). The cells were treated with 60 μM CuIIa for 1, 2, 3, 4, and 5 h respectively. DMSO treatments were used as controls. Data are from three independent duplicates per treatment and the expression level was referenced to GADPH (A) and then further normalized to DMSO treatments (B). The data are presented as $^{\Delta\Delta}$Ct ± SD. The imaginary lines indicate the significant expression level ($^{\Delta\Delta}$Ct ≤ −1 or $^{\Delta\Delta}$Ct ≥ 1).

around 45%. The cycle arrest seemed to be dose-independent.

3.2. CuIIa regulated the expression of genes in EGFR-MAPK pathway

To investigate the effect of CuIIa on the expression of the genes in EGFR-MAPK pathway together with *STAT3* and *survivin*, the A549 cells were treated with CuIIa for 1, 2, 3, 4 and 5 h respectively. The treated cells were then used for RNA extraction. The RNAs were further used for reverse transcription and qPCR analysis. EGFR, Raf1, BRAF, MEK1/2 and ERK1/2 encoding genes were investigated. *Survivin*, the gene encoding symbolic protein involved in tumor cells and the cell cycle regulation gene *cyclinB1* were also examined. The expression levels were referenced to the GADPH encoding gene. All the gene IDs are listed in Table 1. It is common that the regulation of gene expression on transcriptional stage is a fast process that usually happens in a short time, so treatments with 1, 2, 3, 4 and 5 h were tested. As DMSO is reported to be harmful for cells at high concentration, the effect thereof was firstly examined. As shown in Fig. 2A, relative expression ($^{\Delta\Delta}$Ct value) of the most genes was slightly up regulated (*ERK1*. *EGFR*, *ERK2* and *STAT3*) or downregulated (*Raf1*, *BRAF*, *CyclinB1* and *survivin*) compared to the untreated cells except for *MEK1*, *MEK2* and *ERK1*. In most treatments, *MEK1*, *MEK2* and *ERK1* were significantly upregulated, especially *MEK1*. The relative expression of the above genes compared to that of DMSO was shown in Fig. 2B. The expression level shifts of *Raf1*, *BRAF*, *ERK2*, *STAT3* and *survivin* were upregulated in all treatments (especially *Raf1* and *STAT3*), while the expression of *MEK1*, *MEK2*, *ERK1* and *cyclinB1* were downregulated (Notably, *MEK1* and *ERK1*). *EGFR* was an exception and the expression was slightly upregulated under treatment for 3h, and downregulated in other treatments. The expression levels of *Raf1, MEK1*, *ERK1* and *STAT3* was significantly different to DMSO in all CuIIa treatments.

3.3. CuIIa impacted on the accumulation and phosphorylation of members in EGFR-MAPK pathway

Immunoblotting analyses were performed to investigate the accumulation and phosphorylation of the participants in EGFR signaling pathway. EGFR is the first kinase in the pathway, and its activation by binding with ligands triggers the signal transfer (Liu et al., 2018b). Phosphorylation is essential process in EGFR activation (Lemmon and Schlessinger, 2010). As shown in Fig. 3A, the accumulation of EGFR decreased by treatment with CuIIa within 8h, but it increased as time lasted. Although the amount increased after 8h, the phosphorylation level significantly increased under the treatment, and then dropped after 12 h. As kinase activity of EGFR was inhibited by CuIIa (see below), the increase of the pEGFR is supposed to be from the catalysis by other nearby RTKs (Schlessinger, 2000). BRAF and Raf1 are participants located at the fork road in EGFR signaling pathway (Lemmon and Schlessinger, 2010). After the treatment with CuIIa, accumulation of BRAF and Raf1 reduced at the beginning, but the trends inverted after 12 h and 24 h respectively. Interestingly, the phosphorylation of BRAF ascended gradually and continuously while it tended to decrease and touch to the bottom for Raf1 when being treated for 12 h. The possible reason is that the phosphorylation of threonine is not inhibited by CuIIa. The total amount MEK1/2, the direct downstream of Raf remained the same and was not affected by CuIIa, however, its phosphorylation reduced and lasted continuously (Fig. 3B). The accumulation of total and phosphorylated ERK1/2 reached their trough after being treated for 4 h and it increased gradually afterwards (Fig. 3B).

STAT3 transcription factor is an oncogenic driver (Bromberg et al., 1999), and blocking STAT3 results in apoptosis (Cai et al., 2015). As shown in Fig. 3C, the accumulation of STAT3 was reduced within 12 h then recovered to the untreated level. However, the recovery of STAT3 did not complement the consequence of everlasting degrading of survivin, a member of inhibitor of apoptosis protein (IAP) (Li, 2005). CyclinB is essential in cell cycle regulation to promote the cycle from G2 phase to M phase (Westendorf et al., 1989). The absence of cyclinB arrests the cell cycle at G1 phase, however, its continuous accumulation arrests the cycle at G2/M phase. As shown in Fig. 3C, accumulation of cyclinB1 was suppressed in the early treatments, but the suppression was excised in the later treatments. This may help to explain the arrest of cell cycle at G2/M phase (Fig. 1C).

3.4. Kinase activity of EGFR is inhibited by CuIIa

Kinase inhibition assay was performed using the HTRF method to verify whether CuIIa can interfere the kinase activity of EGFR. The inhibition curve simulated is shown in Fig. 4. The result showed that at the concentration of 4 pg·μL^{-1} and upon an incubation of 40 min with 1.6 μM ATP at room temperature, EGFR kinase activity was inhibited by CuIIa, and the 50% inhibition concentration was approximately 1.455 nM. This suggested that CuIIa is a TKI for EGFR with low IC_{50} value that might be a drug candidate for the therapy of EGFR harboring cancers.

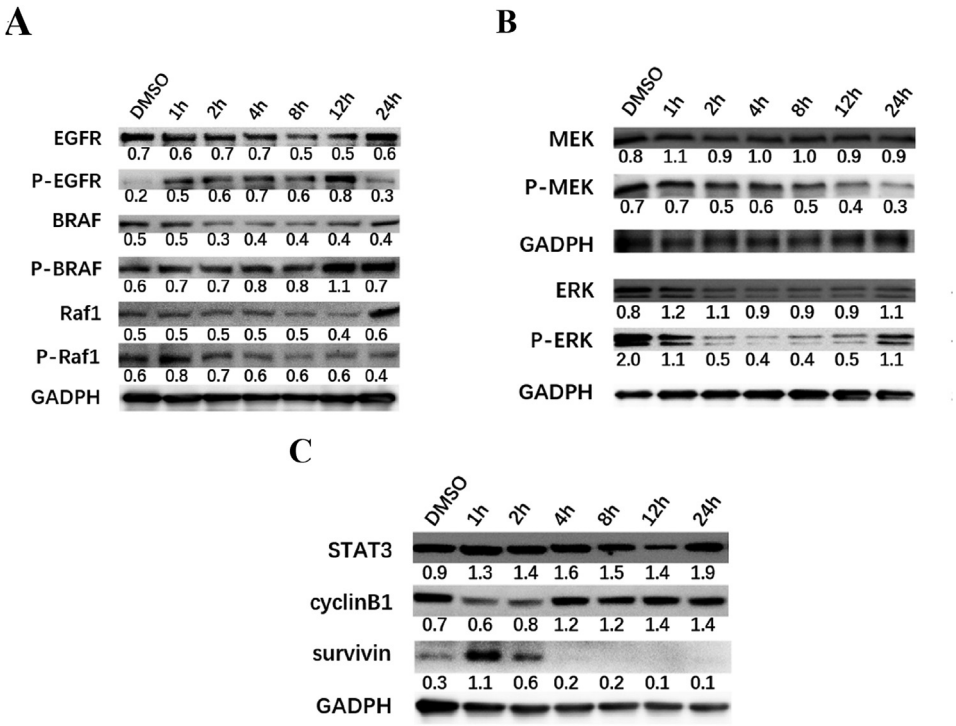

Fig. 3. Impacts of CuIIa to the accumulation of total and phosphorylated proteins. After treated with 60 μM CuIIa for 1, 2, 4, 8, 12, and 24 h, cells were lysed and the lysates were electrophorized and probed with antibodies of (p-)EGFR, (p-)Raf1, (p-)BRAR, (p-)MEK1/2, (p-)ERK1/2, STAT3, survivin, and cyclinB1 to detect the correspondent proteins. The numbers under the blots indicate the gray density ratios of corresponding proteins referenced to those of GADPH.

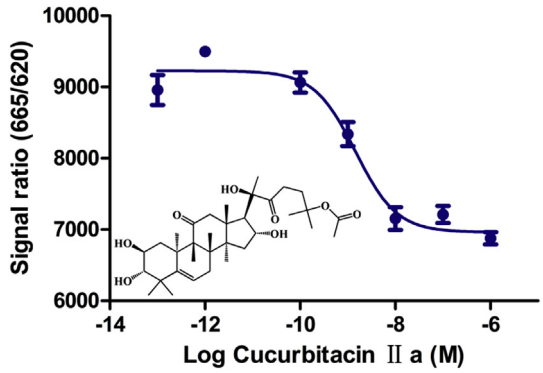

Fig. 4. Structure of CuIIa and the result of the kinase inhibition assay. The curve was achieved with the following reactions: 4 pg·μL^{-1} EGFR, 1.6 μM ATP, and various concentration of CuIIa were mixed and incubated at room temperature for 40 min. Data were presented as mean ± SEM.

3.5. Binding mode between CuIIa and EGFR

In this work, molecular docking was further performed to explore the binding mode of EGFR with CuIIa, whose chemical structure is shown in Fig. 4. The aligned structures of the original X-ray and docked erlotinib have been shown in Fig. 5A. Their principal ring structures almost superimpose each other within the pocket, whereas their flexible side chains protrude out of the surface of EGFR and present different conformations surrounding the entrance of the cavity. Since the highly flexible regions are located outside the protein surface, far away from the active site, they may be assumed to exert negligible influence on the EGFR-erlotinib binding interaction within the pocket. Hence, the docking procedure is reliable and can be employed for investigating the EGFR-CuIIa binding interaction. After validation of the docking procedure, CuIIa was docked into the ATP-binding pocket of EGFR. As shown in Fig. 5B and C, the long side chain of CuIIa occupies the binding pocket and the ligand is stabilized at the active site of EGFR by two hydrogen bonds with Met769. It has been reported that this residue plays a crucial role in stabilizing and enhancing the binding of ligand within the pocket (Stamos et al., 2002), which is consistent with this work. In addition, CuIIa also makes hydrogen bond interactions with Arg817, Thr830, and Asp831 at the active site, thus helping stabilize its position in the pocket. Interestingly, the rigid tetracyclic triterpenoid skeleton of CuIIa is too large to fit into the binding pocket, but instead protrudes out of the pocket and forms a hydrogen bond with Leu694 (Fig. 5B and C).

3.6. Dynamic process of binding between CuIIa and EGFR

In order to assess the binding stability of EGFR-CuIIa complex, their dynamic binding process was performed by MD simulation. The backbone of EGFR shows an increasing fluctuation in the initial simulation and reaches equilibrium after approximately 4 ns (Fig. 6). Similar

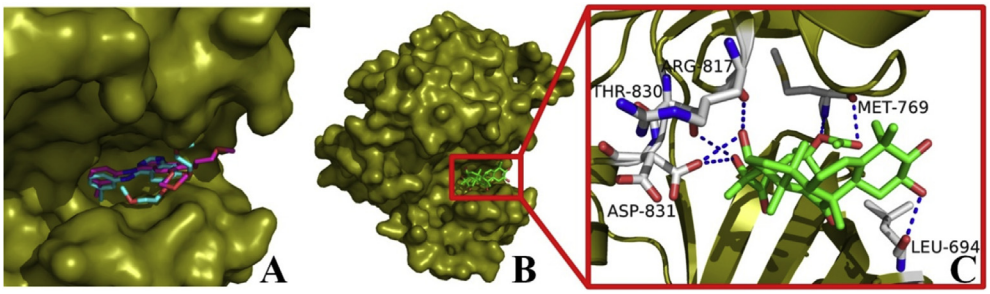

Fig. 5. The results of molecular docking. (A) Docking pose (cyan) and crystallographic pose (magenta) of erlotinib. (B) Docked CuIIa (green) in the binding pocket of EGFR. (C) Hydrogen bond networks between CuIIa (green) and EGFR. (For interpretation of the references to color in this figure legend, the reader is referred to the Web version of this article.)

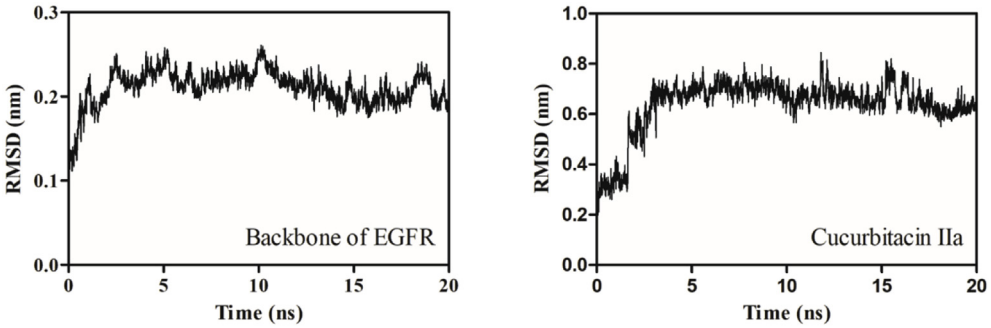

Fig. 6. The variations of root mean square deviation (RMSD) values for the backbone of EGFR (left) and CuIIa (right) during 20-ns MD simulations.

dynamic process of CuIIa has also been observed. The average RMSD values of the backbone of EGFR and CuIIa are 0.21 ± 0.02 and 0.64 ± 0.11 nm respectively, indicating that EGFR remains essentially stable while CuIIa undergoes severe conformational change during the MD simulation. As shown in Fig. 5B, the tetracyclic triterpenoid skeleton of CuIIa protrudes out of the binding pocket, unable to stabilize within the cavity, which may help explain why the conformation of CuIIa exhibits severe fluctuation throughout the simulation.

4. Conclusion

CuIIa inhibits A549 cells proliferation by inducing apoptosis and cell cycle arrest at G2/M phase. The influence of CuIIa on the transcription of the genes involved in EGFR pathway is inconsistent with that on their protein accumulation. The transcription trend of *Raf1* were significantly upregulated while those of *MEK1* and *ERK1* were downregulated significantly in all treatments. The total amount of MEK was constant. On contrast, survivin was completely degraded. On the other hand, phosphorylated Raf1 and MEK decreased continuously while phosphorylated BRAF continuously increased. These destructions of EGFR signaling resulted in abnormal regulated transcription of STAT3 and survivin, and subsequent resulted in apoptosis. The cyclinB1 was slightly downregulated but the accumulation was constant in long time treatment, thus leading to cell cycle arrest at G2/M phase. CuIIa was further confirmed to be a TKI of EGFR with an IC_{50} value of 1.455 nM by kinase inhibition assay. The results of molecular docking show that the long side chain of CuIIa occupies the binding pocket and is stabilized within the cavity. However, the tetracyclic triterpenoid skeleton protrudes out of the pocket, resulting in severe conformational change of CuIIa throughout the MD simulation. By contrast, EGFR is stable without significant conformational change upon binding of CuIIa. Based on the findings above, it is concluded that CuIIa inhibits the proliferation of A549 cells by targeting to EGFR-MAPK signaling pathway.

Declaration of interests

The authors declare that they have no known competing financial interests or personal relationships that could have appeared to influence the work reported in this paper.

Acknowledgements

This work was supported by the National Natural Science Foundation of China (31871717, 31601534 and 31701349), the National Key Research and Development Program of China (2018YFD0300201 and 2016YFD0300103), the China Agricultural Research System (CARS-02-16), and the China Postdoctoral Science Foundation (2018T110249 and 2017M621213).

References

Ahmed, M.S., Halaweish, F.T., 2014. Cucurbitacins: potential candidates targeting mitogen-activated protein kinase pathway for treatment of melanoma. J. Enzym. Inhib. Med. Chem. 29 (2), 162–167.
Alsayari, A., Halaweish, F., Gurusamy, N., 2018. The role of cucurbitacins in combating cancers: a mechanistic review. Pharm. Rev. 12 (24), 157–165.
Arteaga, C.L., 2001. The epidermal growth factor receptor: from mutant oncogene in nonhuman cancers to therapeutic target in human neoplasia. J. Clin. Oncol. 19 (18 Suppl. l), 32s–40s.
Boykin, C., Zhang, G., Chen, Y.H., Zhang, R.W., Fan, X.E., Yang, W.M., Lu, Q., 2011. Cucurbitacin IIa: a novel class of anti-cancer drug inducing non-reversible actin aggregation and inhibiting survivin independent of JAK2/STAT3 phosphorylation. Br. J. Canc. 104 (5), 781–789.
Bromberg, J.F., Wrzeszczynska, M.H., Devgan, G., Zhao, Y., Pestell, R.G., Albanese, C., Darnell, J.E., 1999. Stat3 as an oncogene. Cell 98 (3), 295–303.
Cai, Y., Fang, X., He, C., Li, P., Xiao, F., Wang, Y., Chen, M., 2015. Cucurbitacins: a systematic review of the phytochemistry and anticancer activity. Am. J. Chin. Med. 43 (7), 1331–1350.
Chen, X., Bao, J., Guo, J., Ding, Q., Lu, J., Huang, M., Wang, Y., 2012. Biological activities and potential molecular targets of cucurbitacins: a focus on cancer. Anti Canccer Drugs 23 (8), 777–787.
Cheng, X., Chen, H., 2014. Tumor heterogeneity and resistance to EGFR-targeted therapy in advanced nonsmall cell lung cancer: challenges and perspectives. OncoTargets Ther. 7, 1689–1704.
Chung, H.J., Park, E.J., Pyee, Y., Hua Xu, G., Lee, S.H., Kim, Y.S., Lee, S.K., 2011. 25-Methoxyhispidol A, a novel triterpenoid of Poncirus trifoliata, inhibits cell growth via the modulation of EGFR/c-Src signaling pathway in MDA-MB-231 human breast cancer cells. Food Chem. Toxicol. 49 (11), 2942–2946.
Dong, Q., Yu, P., Ye, L., Zhang, J., Wang, H., Zou, F., Tian, J., Kurihara, H., 2019. PCC0208027, a novel tyrosine kinase inhibitor, inhibits tumor growth of NSCLC by targeting EGFR and HER2 aberrations. Sci. Rep. 9 (1), 5692.
Ellis, L.M., 2004. Epidermal growth factor receptor in tumor angiogenesis. Hematol. Oncol. Clin. N. Am. 18 (5), 1007–1021.
Ganesan, K., Jayachandran, M., Xu, B., 2018. A critical review on hepatoprotective effects of bioactive food components. Crit. Rev. Food Sci. Nutr. 58 (7), 1165–1229.
Garg, S., Kaul, S.C., Wadhwa, R., 2018. Cucurbitacin B and cancer intervention: chemistry, biology and mechanisms (Review). J. Cell. Biochem. 52 (1), 19–37.
He, J., Wang, Y., Xu, L.H., Qiao, J., Ouyang, D.Y., He, X.H., 2013. Cucurbitacin IIa induces caspase-3-dependent apoptosis and enhances autophagy in lipopolysaccharide-stimulated RAW 264.7 macrophages. Int. Immunopharmacol. 16 (1), 27–34.
Hu, Y., Li, Z., Wang, L., Deng, L., Sun, J., Jiang, X., Zhang, Y., Tian, L., Wang, Y., Bai, W., 2017. Scandenolone, a natural isoflavone derivative from Cudrania tricuspidata fruit, targets EGFR to induce apoptosis and block autophagy flux in human melanoma cells. J. Funct. Foods 37, 229–240.
Kampa-Schittenhelm, K.M., Heinrich, M.C., Akmut, F., Rasp, K.H., Illing, B., Dohner, H., Dohner, K., Schittenhelm, M.M., 2013. Cell cycle-dependent activity of the novel dual PI3K-MTORC1/2 inhibitor NVP-BGT226 in acute leukemia. Mol. Cancer 12, 46.
Kaushik, U., Aeri, V., Mir, S.R., 2015. Cucurbitacins - an insight into medicinal leads from nature. Pharm. Rev. 9 (17), 12–18.
Khan, N., Jajeh, F., Khan, M.I., Mukhtar, E., Shabana, S.M., Mukhtar, H., 2017. Sestrin-3 modulation is essential for therapeutic efficacy of cucurbitacin B in lung cancer cells. Carcinogenesis 38 (2), 184–195.
Kim, Y., Lee, B., Shim, J.H., Lee, S.H., Park, W.Y., Choi, Y.L., Sun, J.M., Ahn, J.S., Ahn, M.J., Park, K., 2019. Concurrent genetic alterations predict the progression to target therapy in EGFR-mutated advanced NSCLC. J. Thorac. Oncol. 14 (2), 193–202.
Lee, D.H., 2017. Treatments for EGFR-mutant non-small cell lung cancer (NSCLC): the road to a success, paved with failures. Pharmacol. Ther. 174, 1–21.
Lemmon, M.A., Schlessinger, J., 2010. Cell signaling by receptor tyrosine kinases. Cell 141 (7), 1117–1134.
Li, F., 2005. Role of survivin and its splice variants in tumorigenesis. Br. J. Canc. 92 (2), 212–216.
Li, J., Deng, H., Hu, M., Fang, Y., Vaughn, A., Cai, X., Xu, L., Wan, W., Li, Z., Chen, S., Yang, X., Wu, S., Xiao, J., 2015. Inhibition of non-small cell lung cancer (NSCLC) growth by a novel small molecular inhibitor of EGFR. Oncotarget 6 (9), 6749–6761.
Li, S., Guo, C., Zhao, H., Tang, Y., Lan, M., 2012a. Synthesis and biological evaluation of

4-[3-chloro-4-(3-fluorobenzyloxy)anilino]-6-(3-substituted-phenoxy)pyrimidines as dual EGFR/ErbB-2 kinase inhibitors. Bioorg. Med. Chem. 20 (2), 877–885.
Li, S., Sun, X., Zhao, H., Tang, Y., Lan, M., 2012b. Discovery of novel EGFR tyrosine kinase inhibitors by structure-based virtual screening. Bioorg. Med. Chem. Lett 22 (12), 4004–4009.
Liang, J., Chen, D., 2019. Advances in research on the anticancer mechanism of the natural compound cucurbitacin from Cucurbitaceae plants: a review. Tradit. Med. Res. 4 (2), 68–81.
Liu, J., Liu, X., Ma, W., Kou, W., Li, C., Zhao, J., 2018a. Anticancer activity of cucurbitacin-A in ovarian cancer cell line SKOV3 involves cell cycle arrest, apoptosis and inhibition of mTOR/PI3K/Akt signaling pathway. J.B.U.O.N. 23 (1), 124–128.
Liu, Q., Yu, S., Zhao, W., Qin, S., Chu, Q., Wu, K., 2018b. EGFR-TKIs resistance via EGFR-independent signaling pathways. Mol. Cancer 17 (1), 53.
Lopez-Haber, C., Kazanietz, M.G., 2013. Cucurbitacin I inhibits Rac1 activation in breast cancer cells by a reactive oxygen species-mediated mechanism and independently of Janus tyrosine kinase 2 and P-Rex1. Mol. Pharmacol. 83 (5), 1141–1154.
Mahnashi, M., Elgazwi, S.M., Ahmed, M.S., Halaweish, F.T., 2019. Cucurbitacins inspired organic synthesis: potential dual inhibitors targeting EGFR – MAPK pathway. Eur. J. Med. Chem. 173, 294–304.
Martinelli, E., Morgillo, F., Troiani, T., Ciardiello, F., 2017. Cancer resistance to therapies against the EGFR-RAS-RAF pathway: the role of MEK. Cancer Treat Rev. 53, 61–69.
Masri, M., McManus, M., Mudad, R., 2018. Treatment of advanced non-small cell lung cancer in the era of targeted therapy. Curr. Pulm. Rep. 7 (3), 79–91.
Nakai, K., Hung, M.C., Yamaguchi, H., 2016. A perspective on anti-EGFR therapies targeting triple-negative breast cancer. Am. J. Cancer. Res. 6 (8), 1609–1623.
Padfield, E., Ellis, H.P., Kurian, K.M., 2015. Current therapeutic advances targeting EGFR and EGFRvIII in glioblastoma. Front. Oncol. 5, 5.
Price, K.R., Johnson, I.T., Fenwick, G.R., 1987. The chemistry and biological significance of saponins in foods and feedingstuffs. Crit. Rev. Food Sci. Nutr. 26 (1), 27–135.
Rotow, J., Bivona, T.G., 2017. Understanding and targeting resistance mechanisms in NSCLC. Nat. Rev. Canc. 17 (11), 637–658.
Saada-Bouzid, E., Le Tourneau, C., 2019. Beyond EGFR targeting in SCCHN: angiogenesis, PI3K, and other molecular targets. Front. Oncol. 9, 74.
Schlessinger, J., 2000. Cell signaling by receptor tyrosine kinases. Cell 103, 211–225.
Seo, C.R., Yang, D.K., Song, N.J., Yun, U.J., Gwon, A.R., Jo, D.G., Cho, J.Y., Yoon, K., Ahn, J.Y., Nho, C.W., Park, W.J., Yang, S.Y., Park, K.W., 2014. Cucurbitacin B and cucurbitacin I suppress adipocyte differentiation through inhibition of STAT3 signaling. Food Chem. Toxicol. 64, 217–224.
Stamos, J., Sliwkowski, M.X., Eigenbrot, C., 2002. Structure of the epidermal growth factor receptor kinase domain alone and in complex with a 4-anilinoquinazoline inhibitor. J. Biol. Chem. 277 (48), 46265–46272.
Wang, W.D., Liu, Y., Su, Y., Xiong, X.Z., Shang, D., Xu, J.J., Liu, H.J., 2017. Antitumor and apoptotic effects of cucurbitacin a in A-549 lung carcinoma cells is mediated via G2/M cell cycle arrest and m-TOR/PI3K/AKT signalling pathway. Afr. J. Tradit., Complementary Altern. Med. 14 (2), 75–82.
Westendorf, J.M., Swenson, K.I., Ruderman, J.V., 1989. The role of cyclin B in meiosis I. J. Cell Biol. 108 (4), 1431–1444.
Wheeler, D.L., Huang, S., Kruser, T.J., Nechrebecki, M.M., Armstrong, E.A., Benavente, S., Gondi, V., Hsu, K.T., Harari, P.M., 2008. Mechanisms of acquired resistance to cetuximab: role of HER (ErbB) family members. Oncogene 27 (28), 3944–3956.
Wu, J., Wu, Y., Yang, B.B., 2002. Anticancer activity of Hemsleya amabilis extract. Life Sci. 71 (18), 2161–2170.
Yar Saglam, A.S., Alp, E., Elmazoglu, Z., Menevse, S., 2016. Treatment with cucurbitacin B alone and in combination with gefitinib induces cell cycle inhibition and apoptosis via EGFR and JAK/STAT pathway in human colorectal cancer cell lines. Hum. Exp. Toxicol. 35 (5), 526–543.
Yarden, Y., Sliwkowski, M.X., 2001. Untangling the ErbB signalling network. Nat. Rev. Mol. Cell Biol. 2 (2), 127–137.
Zhou, J., Zhao, T., Ma, L., Liang, M., Guo, Y.J., Zhao, L.M., 2017. Cucurbitacin B and SCH772984 exhibit synergistic anti-pancreatic cancer activities by suppressing EGFR, PI3K/Akt/mTOR, STAT3 and ERK signaling. Oncotarget 8 (61), 103167–103181.
Zubair, M.S., Anam, S., Khumaidi, A., Susanto, Y., Hidayat, M., Ridhay, A., 2016. Molecular docking approach to identify potential anticancer compounds from Begonia (Begonia sp). AIP Conf. Proc. 1755 (1) 080005.